Inorg. Chem. **2003**, *42*, 4864–4872

Synthesis, Characterization, and Evaluation of [Ir(ppy)$_2$(vpy)Cl] as a Polymer-Bound Oxygen Sensor

Maria C. DeRosa,[†] Peter J. Mosher,[†] Glenn P. A. Yap,[‡] K.-S. Focsaneanu,[‡] Robert J. Crutchley,[†] and Christopher E. B. Evans*[,§]

Ottawa-Carleton Chemistry Institute, Ottawa, Ontario, Canada, and the National Research Council of Canada, Ottawa, Ontario, Canada

Received December 3, 2002

This study reports new luminescent oxygen sensors in which the luminophore is covalently bound to the polymer matrix and compares their behavior to related sensors in which the luminophore is dispersed within the matrix. The cyclometalated iridium complex [Ir(ppy)$_2$(vpy)Cl], **1**, has been synthesized and characterized spectroscopically (absorption and emission) and by 1-D and 2-D ^{1}H NMR, elemental analysis, and X-ray crystallography. Complex **1** was attached via hydrosilation to hydride-terminated poly(dimethylsiloxane) (PDMS), yielding material **2**. Successful luminophore attachment was determined spectroscopically from the emission properties, and through the altered physical behavior of **2** compared to a dispersion of **1** in PDMS. Hydrosilation of **1** with dimethylphenylsilane yielded [Ir(ppy)$_2$(DMPSEpy)Cl], **3**, which was fully characterized and used to probe the effect of hydrosilation on the spectroscopic properties of the luminophore. Evaluation of **2** as a luminescent oxygen sensor revealed significantly improved sensitivity over dispersions of **1** in PDMS. Material **2** was also blended with polystyrene (PS) to improve the physical properties of the sensor films. The blend sensors exhibited increased sensitivity relative to films of **2** alone and maintained short response times to rapid changes in air pressure. In contrast, **1** partitioned into the PS phase when dispersed in a PDMS/PS blend, resulting in longer sensor response times.

Introduction

Luminescent oxygen sensors find applications in a variety of uses ranging from in vivo[1] or other biological measurements[2] to monitoring groundwater oxygen levels[3] to luminescence barometry[4] for flow visualization in the automotive and aerospace industries.[5] The sensors do not consume analyte as part of their functioning and can provide an extremely rapid response. Both of these features make them advantageous over electrochemical methods for measuring oxygen.[2d]

The sensors work on the principle of luminescence quenching by oxygen,[6] in which bimolecular collisions between excited luminophores and ground state (triplet) oxygen relax the luminophore nonradiatively, producing singlet oxygen. The relationship between the luminophore's emission intensity, I, or excited state lifetime, τ, and oxygen

* Corresponding author. E-mail: chris.evans@coven.net.
[†] Carleton University, 1125 Colonel By Drive, Ottawa, ON, K1S 5B6 Canada.
[‡] University of Ottawa, 10 Marie Curie, Ottawa, ON, K1N 6N5 Canada.
[§] Institute for Aerospace Research, 1200 Montreal Rd., Ottawa, ON, K1A 0R6 Canada.

(1) Representative examples include: (a) Stücker, M.; Schulze, L.; Pott, G.; Hartmann, P.; Lübbers, D. W.; Röchling, A.; Altmeyer, P. *Sens. Actuators, B* **1998**, *51*, 171−173. (b) Hsu, L.; Heitzmann, H. U.S. Patent 4,712,865, 1987.
(2) See for example: (a) Tyystjärvi, E.; Karunen, J.; Lemmetyinen, H. *Photosynth. Res.* **1998**, *56*, 223−227. (b) Holst, G.; Grunwald, B. *Sens. Actuators, B* **2001**, *74*, 78−90. (c) Navarro-Villoslada, F.; Orellana, G.; Moreno-Bondi, M. C.; Vick, T.; Driver, M.; Hildebrand, G.; Liefeith, K. *Anal. Chem.* **2001**, *73*, 5150−5156. (d) Xu, H.; Aylott, J. W.; Kopelman, R.; Miller, T. J.; Philbert, M. A. *Anal. Chem.* **2001**, *73*, 4124−4133.
(3) (a) McDonagh, C.; Kolle, C.; McEvoy, A. K.; Dowling, D. L.; Cafolla, A. A.; Cullen, S. J.; MacCraith, B. D. *Sens. Actuators, B* **2001**, *74*, 124−130. (b) McDonagh, C.; MacCraith, B. D.; McEvoy, A. K. *Anal. Chem.* **1998**, *70*, 45−50.
(4) For general background information on luminescence barometry, see: (a) Bell, J. H.; Schairer, E. T.; Hand, L. A.; Mehta, R. D. *Annu. Rev. Fluid Mech.* **2001**, *33*, 155−206. (b) Gouterman, M., *J. Chem. Educ.* **1997**, *74*, 697−702. (c) McLachlan, B. G.; Bell, J. H. *Exp. Therm. Fluid Sci.* **1995**, *10*, 470−485. (d) Abbitt, J. D.; Fuentes, C. A.; Carroll, B. F. *Opt. Lett.* **1996**, *21*, 1797−1799.
(5) For examples of applications: (a) Hubner, J. P.; Caroll, B. F.; Schanze, K. S.; Ji, H. F.; Holden, M. S. *AIAA J.* **2001**, *39*, 654−659. (b) Engler, R. H.; Klein, C.; Trinks, O. *Meas. Sci. Technol.* **2000**, *11*, 1077−1085. (c) Taghavi, R.; Raman, G.; Bencic, T. *Exp. Fluids* **1999**, *26*, 481−487. (d) Meier, G. E. A. *Sadhana* **1998**, *23*, 557−567. (e) Dowgwillo, R. M.; Morris, M. J.; Donovan, J. F.; Benne, M. E. *J. Aircr.* **1996**, *33*, 109−116.
(6) Lakowicz, J. R. *Principles of Fluorescence Spectroscopy*; Plenum Press: New York, 1983.

10.1021/ic026230r CCC: $25.00
Published on Web 07/17/2003

concentration is given by the Stern−Volmer equation, eq 1

$$\frac{I^0}{I} = \frac{\tau^0}{\tau} = 1 + K_{SV}[O_2] \quad (1)$$

in which I^0 and τ^0 are, respectively, the luminophore's intensity and lifetime in the absence of oxygen, and K_{SV} is the Stern−Volmer constant. Equation 1 assumes a single luminophore environment, and deviations from the expected linear behavior occur when this is not the case, or when quenching occurs by mechanisms other than bimolecular collisions. In luminescence barometry applications (e.g. wind-tunnel experiments), changes in ambient pressure alter the concentration of dissolved oxygen within the sensor film. Measurements at zero oxygen concentration are often impractical, and it is therefore convenient to use an alternate point of reference, such as $P = 1$ atm. In this case, the relationship between luminescence intensity and air pressure becomes

$$\frac{I_{ref}}{I} = A + Q_S\frac{P}{P_{ref}} \quad (2)$$

in which P_{ref} is the reference pressure at which the luminophore's intensity is I_{ref}. The slope of the Stern−Volmer plot, Q_S, is nominally constrained to values between 0 and 1.[7]

The sensors themselves usually consist of luminophore molecules contained within a gas-permeable matrix such as a polymer or sol−gel glass. The choice of polymer depends largely on the application to which the sensor is intended. Low gas-permeability polymers such as polystyrene (PS) and poly(methyl methacrylate) (PMMA) can be used, but the sensors then have very long response times. Fluorination often increases gas permeability, and polymers such as poly(hexafluoroisopropyl-*co*-heptafluoro-*n*-butyl methacrylate) and poly(2,2,2-trifluoroethyl-*co*-isobutyl methacrylate)[8] are noteworthy as matrix materials. Silicones (polysiloxanes, e.g. poly(dimethylsiloxane), PDMS) were investigated from very early on due to their extremely large gas permeabilities. Unlike high glass transition temperature (T_g) organic polymers such as PS (90 °C) or PMMA (110 °C), many silicones have extremely low T_g's (e.g., PDMS, −127 °C) and thus form films with rather poor mechanical properties unless cured (i.e. cross-linked) or mixed with hardening additives such as silica or alumina.

Commonly used luminophores include polycyclic aromatic hydrocarbons,[9] metalloporphyrins,[10] and polypyridyl transition metal complexes.[11] Sensors based, e.g., on pyrene, PtOEP (OEP = octaethylporphyrin), and $[Ru(dpp)_3]Cl_2$ (dpp = 4,7-diphenylphenanthroline) have all been studied.

The sensors studied to date have predominantly been ones in which the luminescent probe molecules are dispersed within the host matrix as a solid solution. This can lead to problems with the probe molecules aggregating within the matrix or being leached from the matrix, particularly during in vivo or in solvento measurements.[11d,12] If additives or polymer blends are desired to improve the sensor's behavior, the luminophore may partition between the various components leading to complex or unexpected sensor behavior.[7,13] There is, thus, a practical advantage to producing unimolecular sensors in which the luminophores are covalently bound to the matrix.[1b,14]

The choice of methodology for attaching a given luminophore to a given matrix is, of course, very broad. Here we have elected to work with silicones, which have very high gas permeabilities relative to most organic polymers.[15] The main drawback of silicones is that, without curing, they form films with poor mechanical properties. It has also been noted that luminophores such as $[Ru(dpp)_3]Cl_2$ have a strong tendency to aggregate within these matrices,[11d] or to adsorb to the surfaces of rigidifying additives such as silica.[13] To provide mechanical stability to the sensor films, practical silicone-based sensors will need, e.g., to be blended with high T_g polymers. They are thus excellent matrices for investigating the benefits of covalent binding of the luminophore.

Transition metal catalyzed hydrosilation is a convenient method for creating carbon−silicon bonds and was a good candidate reaction for binding our luminophores since a number of relatively inexpensive hydride-containing and hydride-terminated silicone fluids are commercially available.[16] For this synthetic strategy, the luminophore must, of course, be functionalized with a pendent vinyl group to provide a sterically accessible site for the reaction.[17]

As our luminophore we have selected a cyclometalated complex of iridium. The complex $[Ir(ppy)_3]$ (ppy = 2-phen-

(7) Ruffolo, R.; Evans, C. E. B.; Liu, X.-H.; Ni, Y.; Pang, Z.; Park, P.; McWilliams, A. R.; Gu, X.; Lu, X.; Yekta, A.; Winnik, M. A.; Manners, I. *Anal. Chem.* **2000**, *72*, 1894−1904.

(8) (a) Puklin, E.; Carlson, B.; Gouin, S.; Costin, C.; Green, E.; Ponomarev, S.; Tanji, H.; Gouterman, M. *J. Appl. Polym. Sci.* **2000**, *77*, 2795−2804. (b) Subramanian, C. S.; Amer, T. R.; Oglesby, D. M.; Burkett, C. G., Jr. *AIAA J.* **2002**, *40*, 582−584.

(9) (a) Kneas, K. A.; Xu, W.; Demas, J. N.; DeGraff, B. A. *Appl. Spectrosc.* **1997**, *51*, 1346−1351. (b) Cox, M. E.; Dunn, B. *Appl. Opt.* **1985**, *24*, 2114−2120.

(10) (a) Douglas, P.; Eaton, K. *Sens. Actuators, B* **2002**, *82*, 200−208. (b) Vasil'ev, V. V.; Borisov, S. M. *Sens. Actuators, B* **2002**, *82*, 272−276. (c) DiMarco, G.; Lanza, M. *Sens. Actuators, B* **2000**, *63*, 42−48. (d) Mills, A.; Lepre, A. *Anal. Chem.* **1997**, *69*, 4653−4659. (e) Hartmann, P.; Trettnak, W. *Anal. Chem.* **1996**, *68*, 2615−2620. (f) Preininger, C.; Klimant, I.; Wolfbeis, O. S. *Anal. Chem.* **1994**, *66*, 1841−1846.

(11) (a) Mills, A. *Sens. Actuators, B* **1998**, *51*, 60−68. (b) Mills, A.; Thomas, M. D. *Analyst* **1998**, *123*, 1135−1140. (c) Xu W.; Kneas, K. A.; Demas, J. N.; DeGraff, B. A. *Anal. Chem.* **1996**, *68*, 2605−2609. (d) Klimant, I.; Wolfbeis, O. S. *Anal. Chem.* **1995**, *67*, 3160−3166. (e) Hartmann, P.; Leiner, M. J. P.; Lippitsch, M. E. *Anal. Chem.* **1995**, *67*, 88−93. (f) Di Marco, G.; Lanza, M.; Campagna, S. *Adv. Mater.* **1995**, *7*, 468−471. (g) Carraway, J. N.; Demas, J. N.; DeGraff, B. A.; Bacon, J. R. *Anal. Chem.* **1991**, *63*, 337−342.

(12) (a) Wang, H.; Xu, G.; Dong, S. *Analyst* **2001**, *126*, 1095−1099. (b) Hubner, J. P.; Carroll, B. F.; Schanze, K. S.; Ji, H. F. *Exp. Fluids* **2000**, *28*, 21−28.

(13) Lu, X.; Manners, I.; Winnik, M. A. *Macromolecules* **2001**, *34*, 1917−1927.

(14) (a) Yafuso, M.; Korkowski, P. F.; Mader, R. A.; Yan, C.; Carlock, J. T. U.S. Patent 5,296,381, 1994. (b) Holloway, R. R.; Kiang, T. T. U.S. Patent 5,070,158, 1991.

(15) (a) *The Polymer Handbook*, 3rd ed.; Brandrup, J., Immergut, E. H., Eds.; Wiley: New York, 1989. (b) *Polymer Data Handbook*; Mark, J. E., Ed.; Oxford University Press: New York, 1999.

(16) See for example the catalogue *Silanes, Silicones and Metal-Organics* by Gelest Inc.

(17) Speier, J. L. *Adv. Organomet. Chem.* **1979**, *17*, 407−447.

Chart 1. Structure of $[Ir(ppy)_2(vpy)Cl]$, **1**, Indicating the Numbering Scheme Used in Assigning the ^1H NMR

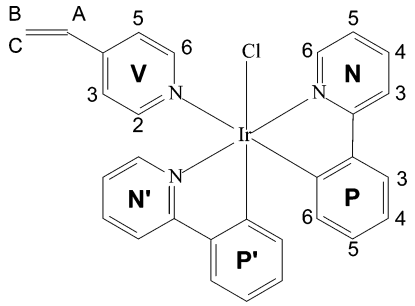

ylpyridine, $\tau^0 = 2\ \mu s$, $\phi = 0.4$)[18a] has previously been examined as a luminescent oxygen sensor,[18] and it provides the advantage over analogous ruthenium complexes such as $[Ru(bipy)_3]Cl_2$ (bipy = 2,2′-bipyridine, $\tau^0 = 0.6\ \mu s$, $\phi = 0.042$)[10d] or $[Ru(phen)_3]Cl_2$ (phen = 1,10-phenanthroline, $\tau^0 = 0.74\ \mu s$, $\phi = 0.08$)[11d] of a longer lifetime and much higher quantum yield. It might be anticipated, in addition, that the nonionic character of such an iridium complex would increase its compatibility in silicone matrices and avoid any deleterious electrostatic interactions with the hydrosilation catalyst. Recent studies of various neutral and ionic cyclometalated iridium complexes have shown many of these complexes to be efficient singlet oxygen photosensitizers.[19]

Herein we report the synthesis, characterization, and evaluation as an oxygen sensor of the nonionic iridium complex $[Ir(ppy)_2(vpy)Cl]$ (vpy = 4-vinylpyridine) (Chart 1). This complex can be readily synthesized from $IrCl_3$ in high yield in two simple steps by cleaving the iridium dimer $[Ir(ppy)_2Cl]_2$ with vinylpyridine, which provides the reactive site for the hydrosilation reaction.

Experimental Section

Methods and Materials. Iridium(III) chloride hydrate was purchased from Strem, 2-phenylpyridine, 4-vinylpyridine, and dimethylphenylsilane were purchased from Aldrich, and Karstedt's catalyst (platinum divinyltetramethyldisiloxane complex in xylene, 2.1−2.4% Pt) and hydride-terminated poly(dimethylsiloxane) (M_n 55000−70000) were purchased from Gelest. 2-Ethoxyethanol (spectrophotometric grade, Aldrich) was used as received, and dichloromethane (laboratory grade, Caledon) was either used as received or dried over calcium hydride (Aldrich) and distilled and stored under nitrogen before use. Toluene (spectrophotometric grade, Caledon) and acetonitrile (reagent grade, Caledon) for spectroscopy were dried over sodium metal and calcium hydride, respectively, and were distilled under nitrogen before use. $[Ir(ppy)_2Cl]_2$ was prepared according to Watts.[20]

Absorption spectra were acquired in dry CH_2Cl_2 on a Cary 5 UV−vis−NIR spectrophotometer at ambient temperatures using quartz cells of either 1.000 (Wilmad) or 0.200 (Hellma) cm path length. Emission spectra were acquired on a Shimadzu RF-1501 spectrofluorometer at ambient temperatures using 1.000 cm path length quartz fluorimeter cells (Wilmad). To obtain time-resolved fluorescence decays, the samples were excited with the third harmonic of a Surelite Nd:YAG laser generating pulses at 355 nm of 6 ns duration and ≤25mJ energy. The signals from the monochromator/photomultiplier system were initially captured by a Tektronix 2440 digitizer and transferred to a Power Macintosh computer with software developed in the LabVIEW environment from National Instruments. A total of four shots were averaged to obtain the decay traces. All experiments were done in static 0.7 × 0.7 cm^2 fused silica cuvettes, following purging with N_2 gas for 15 min. For the quantum yield determinations, the N_2 purged samples were optically matched to an $Ir(ppy)_3$ standard using a Varian Cary 1E spectrophotometer. The steady-state emission was obtained using a Photon Technology International version 1.23 luminescence spectrometer. Fused silica cuvettes (Luzchem Research, Morin Heights, Quebec, Canada) with a 1.0 cm optical path were employed in these experiments. Toluene was used as the solvent for all lifetime and quantum yield measurements except for the lifetime of **3** which was acquired in acetonitrile. NMR spectra were acquired on a Bruker AMX-400 at ambient temperatures using #512 sample tubes (Wilmad) in CD_2Cl_2 or d_6-acetone from Canadian Isotopes Limited and were referenced to solvent resonances or TMS. $[Cr(acac)_3]$ relaxation agent was used to enhance the signal in the ^{29}Si NMR. Elemental analyses were performed by Canadian Microanalytical Service, Ltd. of Delta, BC, Canada. Evaluation of sensor behavior is described in subsequent paragraphs.

Synthesis of $[Ir(ppy)_2(vpy)Cl]$, 1. 4-Vinylpyridine (0.05 mL, 0.46 mmol, fw 105.14 g·mol^{-1}) was added to $[Ir(ppy)_2Cl]_2$ (0.25 g, 0.23 mmol, fw 1072.11 g·mol^{-1}) in dichloromethane (20 mL), and the resultant solution was refluxed under nitrogen for 3 days. After the solution was cooled to RT, toluene (20 mL) was added, the volume was reduced to 20 mL, and the solution was cooled for several hours in a freezer. The yellow microcrystalline product was collected by suction filtration, rinsed with 5 mL aliquots of toluene and hexanes, and dried in vacuo. $[Ir(ppy)_2(vpy)Cl]$ (0.21 g, 0.33 mmol, 70% yield, fw 641.19 g·mol^{-1}) elemental analysis as the monohydrate $C_{29}H_{23}ClIrN_3 \cdot H_2O$ calcd (%): C 52.68, H 4.12, N 6.35. Found: C 53.01, H 3.74, N 5.93. ^1H NMR (CD_2Cl_2, 400 MHz): 9.77 (N6, 1H, d, 5.8 Hz), 8.8 (V2,6, 2H, br), 8.04 (N6′, 1H, d, 5.8 Hz), 7.85 (N3′, 1H, d, 7.9 Hz), 7.70 (N3, 1H, m), 7.65 (N4′, 1H, m), 7.64 (N4, 1H, m), 7.51 (P3′, 1H, dd, 7.7 Hz), 7.46 (P3, 1H, dd, 7.7 Hz), 7.15 (N5, 1H, m), 7.12 (V3,5, 2H, br), 7.00 (N5′, 1H, ddd, 6.6 Hz), 6.81 (P4, 1H, ddd, 7.5 Hz), 6.76 (P4′, 1H, ddd, 7.5 Hz), 6.71 (P5, 1H, ddd, 7.4 Hz), 6.64 (P5′, 1H, ddd, 7.4 Hz), 6.53 (VA, 1H, dd, 17.6 10.9 Hz), 6.25 (P6, 1H, d, 7.6 Hz), 6.08 (P6′, 1H, d, 7.6 Hz), 5.91 (VC, 1H, d, 17.6 Hz), 5.46 (VB, 1H, d, 10.9 Hz) ppm. UV−vis ϵ_{261} 4.00 × 10^4, ϵ_{396} 4.44 × 10^3 L·mol^{-1}·cm^{-1}.

Synthesis of $[Ir(ppy)_2(DMPSEpy)Cl]$, 3. Dimethylphenylsilane (50 μL, 0.33 mmol, fw 136.27 g·mol^{-1}) was added to a solution of **1** (100 mg, 0.16 mmol, fw 641.19 g·mol^{-1}) in CH_2Cl_2 (12 mL) with Karstedt's catalyst (20 μL, 2.1% Pt solution in xylenes, ca. 1% relative to vinyl). The resultant solution was refluxed under nitrogen for 24 h. The product was then slightly concentrated and precipitated into hexanes to remove unreacted silane. The yellow precipitate was collected by suction filtration and purified by column chromatography on silica gel using 2:1 hexanes/acetone as the mobile phase, collecting the first yellow band. The eluate was solvent stripped to dryness and the yellow product dried in vacuo.

(18) (a) Vander Donckt, E.; Camerman, B.; Hendrick, F.; Herne, R.; Vandeloise, R. *Bull. Soc. Chim. Belg.* **1994**, *103*, 207−211. (b) Amao, Y.; Ishikawa, Y.; Okura, I. *Anal. Chim. Acta* **2001**, *445*, 177−182.
(19) (a) Di Marco, G.; Lanza, M.; Mamo, A.; Stefio, I.; Di Pietro, C.; Romeo, G.; Campagna, S. *Anal. Chem.* **1998**, *70*, 5019−5023.(b) Di Marco, G.; Lanza, M.; Pieruccini, M.; Campagna, S. *Adv. Mater.* **1996**, *8*, 576−580. (c) Gao, R.; Ho, D. G.; Hernandez, B.; Selke, M.; Murphy, D.; Djurovich, P. I.; Thompson, M. E. *J. Am. Chem. Soc.* **2002**, *124*, 14828−14829.
(20) Sprouse, S.; King, K. A.; Spellane, P. J.; Watts, R. J. *J. Am. Chem. Soc.* **1984**, *106*, 6647−6653.

[Ir(ppy)$_2$(DMPSEpy)Cl] (31 mg, 0.04 mmol, 25% yield, fw 777.46 g·mol^{-1}) elemental analysis as the monohydrate $C_{37}H_{35}ClIrN_3Si\cdot H_2O$ calcd (%): C 55.87, H 4.69, N 5.28. Found: C 55.49, H 4.45, N 5.16. ^{1}H NMR (CD_2Cl_2, 400 MHz): 9.85 (N6, 1H, d, 5.2 Hz), 8.8 (V2,6, 2H, br), 8.10 (N6′, 1H, d, 5.1 Hz), 7.92 (N3′, 1H, d, 8.3 Hz), 7.78 (N3, 1H, m), 7.74 (N4′, 1H, m), 7.72 (N4, 1H, m), 7.60 (P3′, 1H, dd, 7.8 Hz), 7.54 (P3, 1H, dd, 7.7 Hz), 7.48 (Si-*Ph*, 1H, m), 7.34 (Si-*Ph*, 2H, m) 7.23 (N5, 1H, m), 7.07 (N5′, 1H, m), 7.02 (V3,5, 2H, br), 6.88 (P4, 1H, ddd, 7.5 Hz), 6.84 (P4′, 1H, ddd, 7.6 Hz), 6.78 (P5, 1H, ddd, 7.4 Hz), 6.72 (P5′, 1H, ddd, 7.4 Hz), 6.33 (P6, 1H, d, 7.6 Hz), 6.16 (P6′, 1H, d, 7.6 Hz), 2.54 (CH_2CH_2Si, 2H, m), 1.03 (CH_2CH_2Si, 2H, m), 0.26 (Si-CH_3, 6H, s). ^{29}Si (d_6-acetone, 80 MHz): −5.8 ppm. UV−vis ϵ_{262} 4.97 × 10^4, ϵ_{399} 4.75 × 10^3 L·mol^{-1}·cm^{-1}.

Synthesis of 2 by Attachment of 1 to Hydride-Terminated PDMS. A solution of **1** (50 mg, 0.08 mmol, fw 641.19 g·mol^{-1}) in CH_2Cl_2 (5 mL) was added to a solution of hydride-terminated PDMS (4 g, 0.06 mmol, Mn = 55−70 kDa) in CH_2Cl_2 (10 mL) with Karstedt's catalyst (10 μL, 2.1% Pt solution in xylenes, ca. 1% relative to vinyl). The resultant solution was stirred at reflux under nitrogen for 2 days and the solvent stripped to dryness. The product was dissolved in a small volume of hexanes and was filtered through a 1.0 μm Gelman Acrodisc to remove unreacted complex. A clear, yellow solid was obtained by dropwise addition of the filtered solution to rapidly stirred methanol.

Dissolution/Precipitation of a Mixture of 1 and PDMS. A mixture of solid **1** and hydride-terminated PDMS was dissolved in CH_2Cl_2 to form a homogeneous solution which was subsequently solvent stripped to dryness resulting in a cloudy yellowish suspension of complex in polymer. Dissolution of the mixture in hexanes resulted in a cloudy solution from which, after microfiltration through a 1.0 μm Gelman Acrodisc, was obtained a clear, colorless silicone fluid.

X-ray Structural Determination of 1·$(CH_3CH_2)_2O$. A suitable crystal was selected, mounted on a thin glass fiber using paraffin oil, and cooled to the data collection temperature. Data were collected on a Bruker AXS SMART 1k CCD diffractometer using 0.3° ω-scans at 0°, 90°, and 180° in φ. Initial unit-cell parameters were determined from 60 data frames collected at different sections of the Ewald sphere. Semiempirical absorption corrections based on equivalent reflections were applied.[21]

Systematic absences in the diffraction data and unit-cell parameters were uniquely consistent with the reported space group. The structure was solved by direct methods, completed with difference Fourier syntheses, and refined with full-matrix least-squares procedures based on F^2. A molecule of diethyl ether solvent was found cocrystallized in the asymmetric unit. All nonhydrogen atoms were refined with anisotropic displacement coefficients. All hydrogen atoms were treated as idealized contributions. All scattering factors are contained in the SHELXTL 6.12 program library.[22]

Determination of Quenching Sensitivity to Oxygen, (Q_S). Measurements were performed on samples of **2** and 1:1 and 1:9 **2**/PS blends, as well as on dispersions of **1** and **3** in PDMS, PS, and 1:1 PDMS/PS blends. Samples of **2** were applied using toluene as the solvent, whereas samples of **1** and **3** were applied using CH_2Cl_2 due to the poor solubility of the free luminophores in toluene.

Each sample was treated as follows: A solution of the sample was applied to an aluminum plate previously covered with a layer of Tristar Starpoxy fluid resistant white epoxy primer (DHMS C4.01 Ty3) using a conventional airbrush. The painted plate was then mounted in an in-house designed pressure chamber. Pressure was controlled via a Scanivalve Corp model PCC100 pressure calibrator/controller, and the temperature of the mounting plate was controlled via a thermoelectric cooler coupled to a model LFI-3551 temperature controller using a model TCS650 thermistor in the 10 μA range, both from Wavelength Electronics. Excitation was provided by a Hamamatsu Lightningcure LC5 200W model L8333 Hg/Xe source via a 10 m × 8 mm Oriel UV−vis liquid light guide (transmission window 300−650 nm). The source was equipped with 011FG09 and 300FS40 filters from Melles-Griot, transmitting approximately in the range 280−320 nm. Emission was measured by a 512 × 512 Photometrics CH350 12-bit CCD camera equipped with a 500 ± 40 nm band-pass filter (500FS80−50, Melles Griot). Measurements were taken at 10 °C, scanning from low to high pressure. At each pressure, multiple measurements were taken to ensure the oxygen concentration in the film had come to equilibrium. The time required for this to occur provided a qualitative measure of response time. At the end of each calibration, a second reading at 15 psi was taken to ensure no significant photodegradation had occurred on the time scale of the experiment. Backgrounds were measured on a section of primed plate. Spectra were also collected for various calibrations using an Acton Research Corporation SpectruMM CCD detection system. A fiber optic lightguide (LG-455-020) equipped with a Kodak #3 gelatin filter passed the emission through a SpectraPro-150 imaging dual grating monochromator/spectrograph onto a 16-bit Hamamatsu 1024 × 256 CCD.

Results and Discussion

Syntheses. The synthetic transformations of this study are outlined in Scheme 1.

Complex **1** was synthesized by reacting 4-vinylpyridine with the chloride-bridged iridium dimer [Ir(ppy)$_2$Cl]$_2$ in a manner similar to that of Nonoyama.[23] Successful synthesis of **1** was monitored by the appearance in the ^{1}H NMR spectrum of the characteristic resonances for the vinyl protons of 4-vinylpyridine, and through the increased complexity of the aromatic region. Use of COSY and NOESY 2-D techniques allowed for individual assignment of each hydrogen of both phenylpyridine ligands and the vinylpyridine ligand. Proton assignments to a given ppy ligand are accurate, but it was not possible to determine which ppy (primed or unprimed) was *trans* to vpy. The structure was confirmed by X-ray crystallography, and the ORTEP of **1**·$(CH_3CH_2)_2O$ is given as Figure 1. Tables 1 and 2 contain crystallographic data and selected bond lengths and angles, respectively. The Ir−N and Ir−C bond lengths for the ppy ligands are in accord with similar species containing an [Ir(ppy)$_2$] fragment.[24a,25] The vpy Ir−N bond is significantly longer than the Ir−N bonds for the ppy ligands. This is to be expected since the ppy nitrogens sit *trans* to each other whereas the vpy nitrogen is *trans* to a ppy carbon and not part of a metallocycle. The vpy Ir−N bond is slightly longer (by ca. 0.07 Å) than a ppy Ir−N bond length for a nitrogen *trans* to a carbon atom.[25]

(21) Blessing, R. *Acta Crystallogr*. **1995**, *A51*, 33−38.
(22) Sheldrick, G. M. Bruker AXS, Madison, WI, 2001.
(23) (a) Nonoyama, M. *Bull. Chem. Soc. Jpn.* **1974**, *47*, 767−768. (b) Nonoyama, M. *J. Organomet. Chem.* **1974**, *82*, 271−276.
(24) (a) Lamansky, S.; Djurovich, P.; Murphy, D.; Abdel-Razzaq, F.; Kwong, R.; Tsyba, I.; Bortz, M.; Mui, B.; Bau, R.; Thompson, M. E. *Inorg. Chem.* **2001**, *40*, 1704−1711. (b) Lamansky, S.; Djurovich, P.; Murphy, D.; Abdel-Razzaq, F.; Lee, H.-E.; Adachi, C.; Burrows, P. E.; Forrest, S. R.; Thompson, M. E. *J. Am. Chem. Soc.* **2001**, *123*, 4304−4312.
(25) Colombo, M. G.; Brunold, T. C.; Riedener, T.; Güdel, H. U.; Förtsch, M.; Bürgi, H.-B. *Inorg. Chem.* **1994**, *33*, 545−550.

Scheme 1

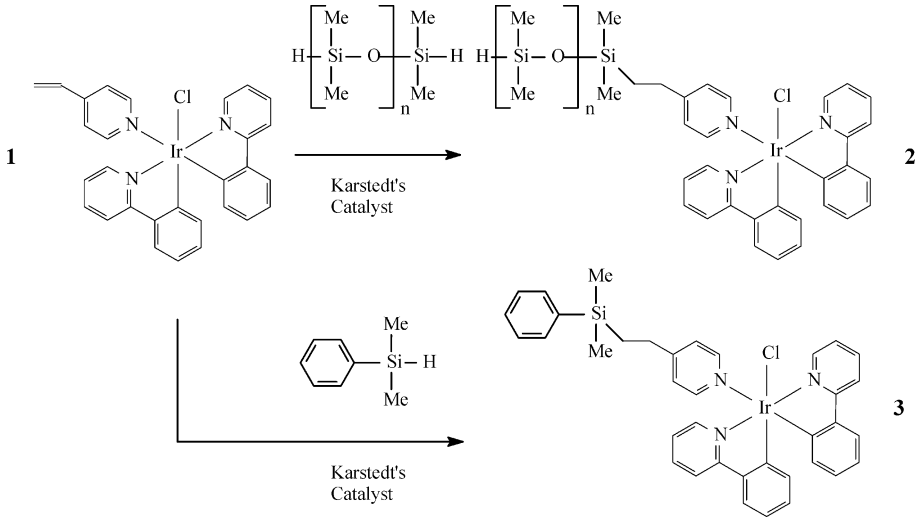

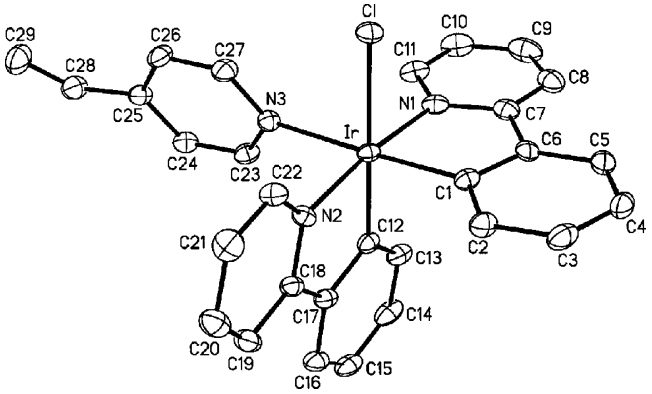

Figure 1. ORTEP of **1**·$(CH_3CH_2)_2O$ with thermal ellipsoids depicted at 30% probability. The diethyl ether molecule of solvation and all hydrogen atoms have been omitted for clarity.

Table 1. X-ray Crystallographic Data for **1**·$(CH_3CH_2)_2O$

empirical formula	$C_{33}H_{33}ClIrN_3O$
fw	715.27
cryst syst	monoclinic
space group	$P2_1/n$
unit cell dimensions	$a = 16.4774(19)$ Å
	$b = 10.7471(13)$ Å
	$c = 17.489(2)$ Å
	$\beta = 113.210(2)°$
V	2846.4(6) Å^3
d_{calcd}	1.669 g/cm^3
T	203(2) K
λ	0.71073 Å
R1 (F_o^2)	0.0354
wR2 (F_o^2)	0.1099
Z	4
abs coeff	4.816 mm^{-1}

Reaction between **1** and hydride-terminated PDMS (Mn 55−70 kDa) resulted in luminophore-end-functionalized PDMS, **2**. For exhaustive luminophore loading, treating **2** as a solution of **1** in PDMS, the maximum concentration range of **1** is 35.3−27.7 mM (23000−18000 ppm). The actual concentration of attached luminophore was assessed spectroscopically using the molar absorptivity of the $\pi-\pi^*$ transition of **3** to model the attached luminophore (see the subsection describing electronic spectroscopy). Accordingly, **2** was found to be 3.6 mM (2400 ppm) in luminophore. From the reaction stoichiometry, 100% attachment would have resulted in a luminophore concentration of 18.9 mM (12500 ppm). The hydrosilation reaction yield is therefore approximately 20%.

Table 2. Selected Bond Lengths (Å) and Angles (deg) for **1**·$(CH_3CH_2)_2O$[a]

Ir−Cl	2.5045(12)	C1−Ir−N3	177.94(17)
Ir−C1	2.004(5)	Cl−Ir−C12	177.41(14)
Ir−N1	2.042(4)	Cl−Ir−N1	88.11(11)
Ir−N3	2.203(4)	Cl−Ir−N2	97.04(11)
C28−C29	1.317(8)	Cl−Ir−N3	90.19(12)
N1−Ir−C1	80.29(18)	C25−C28−C29	125.9(6)
N1−Ir−N2	173.27(15)	N1−Ir−C12	93.83(18)

[a] Standard deviations are given in parentheses.

Due to its low concentration in **2**, NMR could not be used to probe the attached luminophore directly. Luminophore attachment was, however, evident by the different behavior of **2** relative to a dispersion of **1** in PDMS. For example, while PDMS and **2** are both soluble in hexanes, **1** is not. A sample of **2** can thus be wholly dissolved in hexanes, whereas with a dispersion of **1** in PDMS (prepared by solvent stripping a dichloromethane solution of the two components to dryness) only the polymer dissolves, leaving behind a suspension of **1**. Other evidence of successful attachment is discussed in the following subsections on electronic spectroscopy and oxygen sensitivity.

Reaction of **1** with dimethylphenylsilane yielded **3**, which was characterized spectroscopically to probe the effects of hydrosilation on the properties of the luminophore. Complex **3** exhibits a single resonance in the ^{29}Si NMR at −5.8 ppm, as well as an absence of vinyl resonances in its ^{1}H NMR spectrum, suggesting the successful formation of the anticipated Si−C bond from condensation of the vinyl and Si−H moieties.

Electronic Spectroscopy and Photophysical Data. Spectroscopic data for **1**, **2**, and **3** have been placed in Table 3, and representative spectra are given in Figure 2. The absorption spectra of all three were assigned by analogy to similar complexes[20,24,25] and show intense phenyl- and pyridyl-based $\pi-\pi^*$ bands near 260 nm with ^{1}MLCT transitions near 400 nm and ^{3}MLCT transitions near 450 nm.

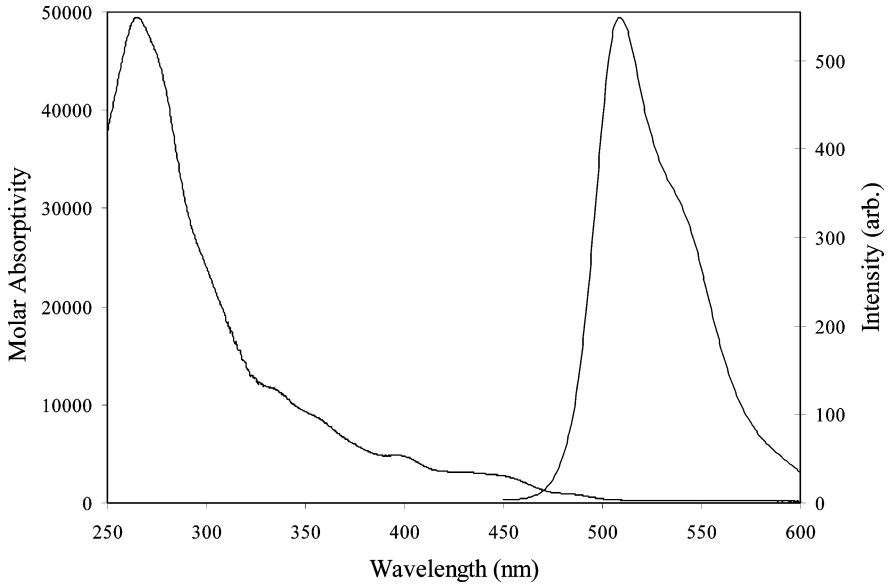

Figure 2. Solution absorption (CH_2Cl_2) and emission (toluene) spectra of **2**. The molar absorptivity has been estimated on the basis of data for **3**. The emission spectrum is uncorrected.

Table 3. Solution Absorption, Emission, and Photophysical Data for **1**, **2**, and **3**

	1	**2**	**3**
λ_{max} $\pi-\pi^{*a}$ (ϵ)^b	261 (4.00×10^4)	265	262 (4.97×10^4)
λ_{max} MLCT (ϵ)	396 (4.44×10^3)	396	399 (4.75×10^3)
λ_{max} emission	506	509	509
λ_{max} emission^c	525^d	537	537
ϕ	0.06	0.32	0.07
τ^{0e}	60^f	190	430

^{a} Wavelengths in nm. ^{b} ϵ has units of L·mol^{-1}·cm^{-1}. ^{c} Low-energy shoulder. ^{d} Not resolved. ^{e} τ^0 has units of ns. ^{f} Approximate (see text).

None of the complexes absorbs significantly at wavelengths longer than 500 nm.

The molar absorptivity of the $\pi-\pi^*$ transition in **3** is significantly larger than in **1**. Adding dilute HCl to a solution of **1** also led to an increase in the intensity of this transition, presumably due to acid hydrolysis of the double bond. We suggest that the loss of the vinyl group and the consequently reduced conjugation of the monodentate pyridyl ligand result in a simplification of electronic transitions, leading to a decrease in bandwidth and an increase in intensity. Since the luminophore in **2** is expected to be electronically similar to that in **3**, the extinction coefficient of **3** was used to calculate the luminophore concentration in **2**. Note that the molar absorptivities shown in Figure 2 are estimates obtained by assuming $\epsilon(\pi-\pi^*)\mathbf{2} = \epsilon(\pi-\pi^*)\mathbf{3}$.

The solution emission spectra of **2** and **3** in toluene have identical band shapes, with maxima at 509 nm and low-energy shoulders at 537 of roughly 60% the intensity of the main band. The emission spectrum of **1**, however, is quite different, exhibiting a single broad band extending from 490 to 550 nm, with a maximum at 506 nm and no well-defined low-energy shoulder. These spectra are available as Figure SI1 in the Supporting Information.

The luminescence lifetimes along with quantum yields for **1**, **2**, and **3** can be found in Table 3. Owing to the extremely low luminescence intensity of **1**, deconvolution of the decay profile was difficult, and the lifetime given in Table 3 for this complex must be considered to be approximate.

The emission spectra of thin films of **2** and dispersions of **1** and **3** in PDMS are given in Figure 3. As with the solution spectra, the thin-film emission band shape of **2** is similar to that of **3** and very different from that of **1**. When PS is used as a blend polymer to rigidify the thin films, changes occur in both band shape and energy, resulting in similar emission profiles for all three species. The spectra in Figure 5 are representative, and a comparison of the thin-film emission spectra of **1** and **3** in PS and 1:9 **2**/PS is given as Figure SI2 in the Supporting Information.

It is tempting to assign the change in emission band shape between **1** and **2** (or **3**) to the differing extent of conjugation of the pyridine ligand. Although this is seemingly supported by the solution and PDMS thin-film data, the similarity of the spectra of all three species in PS suggests this view may be too simplistic.

The emission band shapes of **1** suggest that the luminophore partitions into the PS phase when a 1:1 PDMS/PS blend is used as the matrix. In PDMS, the emission spectrum is broad and featureless (see Figure 3), whereas in PS it exhibits a distinct low-energy shoulder (see Figure SI2). When dispersed in a 1:1 PDMS/PS blend, the emission profile is identical to that of **1** in PS, with no broadening or shifting to lower energy, which would be expected if a significant proportion of the luminophore was in the PDMS phase. The emission spectra of thin films of **3** dispersed in PDMS, PS, and a 1:1 PDMS/PS blend similarly indicate partitioning of the luminophore into the PS phase of the blend. In this case, the change in band shape (see Figures 3 and SI2) occurs at the low-energy shoulder, which is better resolved and of significantly lower intensity in PS compared to PDMS. A similar, but slightly less extensive, change can be observed in the spectra of **2** and its PS blends. The spectral narrowing and changes in band shape that occur in the presence of PS can be attributed to different luminophore

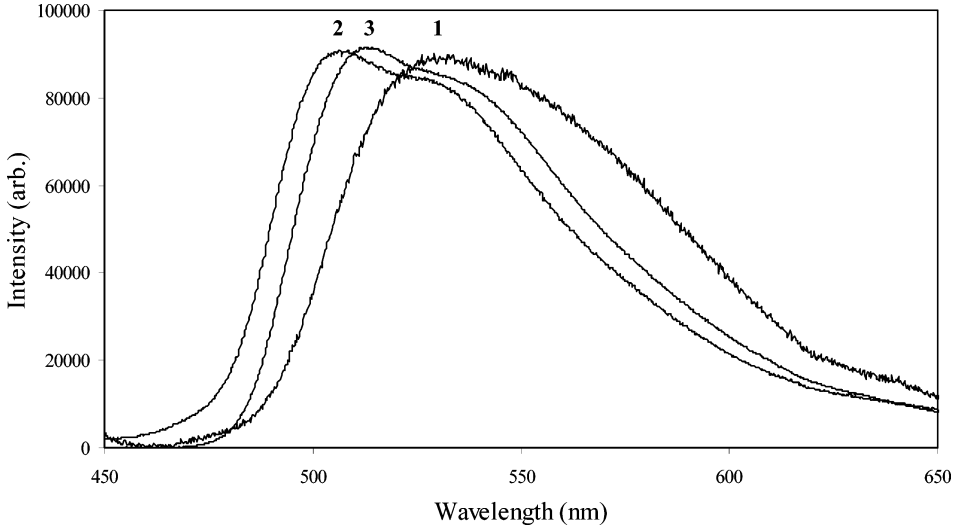

Figure 3. Thin-film emission spectra of **2** and of dispersions of **1** and **3** in PDMS. The spectra have been rescaled to fit the figure, and no significance should be attributed to the relative spectral intensities.

Table 4. Q_S Values (r^2 in Parentheses) from CCD Luminescence Quenching Data over the Pressure Range 0.05−45 psi

	matrix[a]		
	PDMS	1:1 PDMS/PS	PS
1	0.1173[b]	0.0671 (0.9892)	0.0812 (0.9860)
	0.0305 (0.9843)[c]		
2	0.6343[b]	0.5613[b]	0.5867[b]
	0.1554 (0.9948)[d]	0.1199 (0.9882)[c]	0.1519 (0.9875)[c]
	0.08 (0.9978)[e]		
3	0.0329 (0.9926)	0.1362 (0.9997)	0.1678 (0.9926)

[a] For **2**, the matrices are **2**, 1:1 **2**/PS, and 1:9 **2**/PS. [b] 0.05−5 psi. [c] 10−45 psi. [d] 10−20 psi. [e] 25−45 psi.

solvation microenvironments in PS relative to PDMS, and may also be due in part to solvent viscosity effects that have been noted for the ^{3}MLCT emissions of similar species.[25]

Oxygen Sensitivity. Quenching sensitivity (Q_S) data have been placed in Table 4, and representative Stern−Volmer plots are given as Figure 4. Where curvature in the Stern−Volmer plots did not allow an acceptable linear fit ($r^2 > 0.98$) to the data, Q_S values were obtained within constrained presssure ranges that did give linear data fits. The reported data were obtained from CCD experiments. Figure 5 shows the spectral response to changes in pressure. Stern−Volmer plots using the intensity of the spectral band maximum tend to give slightly higher Q_S values than the CCD data, and the CCD data are believed to slightly underrepresent oxygen sensitivity due to the presence of scattered light from the excitation source that could not be completely blocked by the camera's filters.

Oxygen sensitivity of **2** was measured on thin films of **2** itself as well as on films of **2** blended with PS in both 1:1 and 1:9 ratios. These data were compared with measurements on **1** and **3** dispersed in the same hydride-terminated PDMS used in the synthesis of **2**, in PS, and in a 1:1 PDMS/PS blend. The oxygen quenching data support the luminophore partitioning suggested by the electronic spectra.

As shown in Figure 4, the quenching sensitivity of a thin film of **2** is greater than the sensitivity of films of dispersions of **1** or **3** in PDMS, which give nearly equivalent Stern−Volmer plots except for a slight downward curvature in the response of **1** at low ($P < 5$ psi) total pressures. In light of the lifetime data, we ascribe the greater sensitivity of **2** to a decreased tendency for the luminophore to aggregate in this material. The Ir complex in **2** has, by virtue of its being bound to a long PDMS chain, greatly reduced mobility. We suggest the inability of the luminophore to move independently of the polymer chain leads to its diminished tendency to aggregate.

The marked downward curvature of the Stern−Volmer plots of **2** has been seen for transition metal complexes in PDMS by other researchers and has been ascribed to the luminophore being solvated in different microenvironments within the polymer matrix, having different accessibilities to oxygen.[11d,11g,26] Thus, at low pressures only the most accessible luminophore molecules interact with oxygen, leading to high sensitivity, whereas at higher pressures the easily accessible luminophore molecules are largely quenched, and the quenching sensitivity is increasingly dominated by the luminophore molecules in the less accessible domains. Often, the luminescence emission decay profile in these cases can be modeled with two exponentials (luminophore lifetimes), and the downward curvature of the Stern−Volmer plots is then attributed to the "two-site model". This is, of course, a great oversimplification, and it is generally accepted that a range of different solvation microenvironments is likely to occur in any given sample.[11g]

Dispersions of **1** or **3** in PS or 1:1 PDMS/PS blends show increased oxygen sensitivity relative to the dispersions in PDMS alone. For **1**, Q_S is approximately equal in PS or the 1:1 blend, whereas for **3** the quenching sensitivity is greater in pure PS than in the PDMS/PS blend. These data are reflected in the behavior of **2**, where the oxygen sensitivity increases with increasing proportion of PS in the matrix going from pure **2** to 1:1 and 1:9 **2**/PDMS blends. The sensitivities of **3** in PS and 1:9 **2**/PS are very similar, except for the curvature at low pressures of the latter sample.

(26) Demas, J. N.; DeGraff, B. A. *J. Chem. Educ.* **1997**, *74*, 690−695.

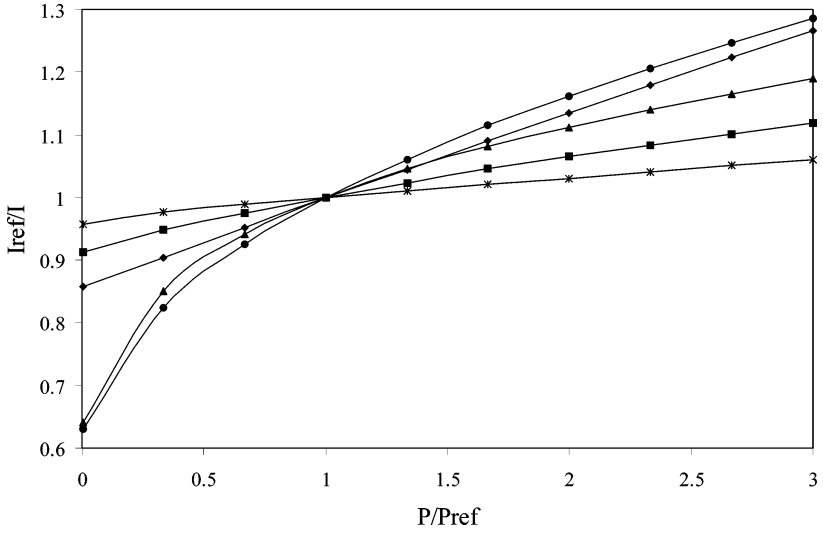

Figure 4. Stern−Volmer calibration curves for films of **3** in PDMS (*), **1** in 1:1 PDMS/PS (■), **2** (▲), **3** in 1:1 PDMS/PS (◆), and 1:9 **2**/PS (●).

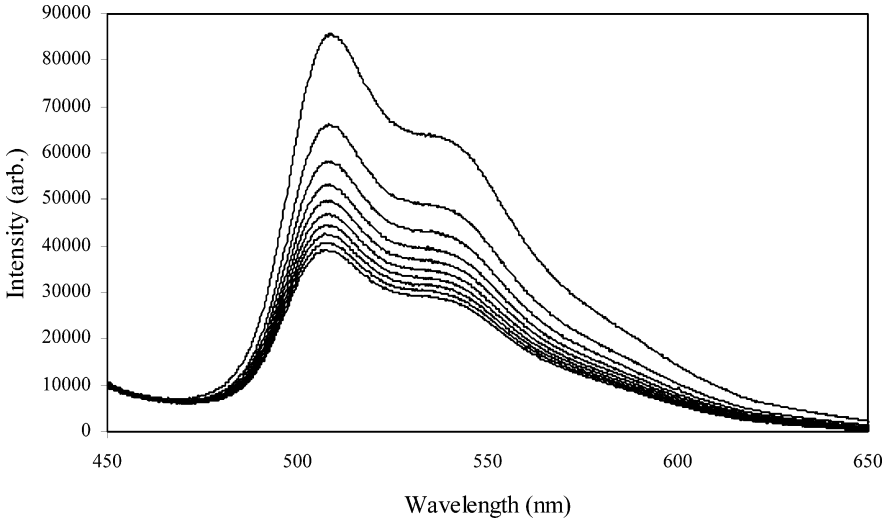

Figure 5. Spectra of a thin film of 1:9 **2**/PS showing the loss of intensity with increasing total air pressure. Spectra were taken at 5 psi increments over the range 0.05−45 psi and have been corrected for background. Q_S from band maxima are 0.556 (0−5 psi) and 0.187 ($r^2 = 0.9938$) in the range 10−45 psi.

The degree of curvature in the Stern−Volmer plots decreases as the proportion of high T_g polymer is increased, presumably due to the limited mobility of the luminophore molecules in the more rigid matrix. This is apparent in the data for **2** and a 1:9 **2**/PS blend shown in Figure 3 and may suggest that the luminophore in the polystyrene blend is solvated by PS at the interface of the two polymers.

Sensor response time is an important criterion for certain applications. Although response times were not measured quantitatively (see Experimental Section), the "dispersed-in-PS" sensors exhibited markedly longer response times to changes in total pressure (on the order of tens of seconds) relative to the "dispersed-in-PDMS" sensors (which responded as quickly as the pressure could be changed). The response times of PS blends of **2** remained very short, however, being at most a few seconds for the 1:9 **2**/PS sensor. Maintaining a short response time in the presence of rigidifying additives is a distinct advantage brought about by attachment of the luminophore.

Conclusion

Luminescent oxygen sensors based on the iridium complex [Ir(ppy)$_2$(vpy)Cl], **1**, have been synthesized via hydrosilation of luminophore **1** onto hydride-terminated PDMS. The luminophore-attached sensors compare favorably, both in sensitivity and versatility, with dispersed sensors utilizing transition metal coordination complexes having similar structures and excited state lifetimes (e.g. $[Ru(bpy)_3]^{2+}$). Not only is the oxygen sensitivity of **2** greater than a dispersion of **1** in PDMS, but the physical properties of the sensor film can be improved by blending without compromising sensor behavior. Blends of **2** with PS yielded robust films which exhibited improved oxygen sensitivity relative to films of **2** alone, while maintaining short response times to changes in oxygen concentration. This is in direct contrast to the effect of blending on the response times of the dispersed luminophore sensors. Preferential solvation of **1** by polystyrene in a PDMS/PS blend led to greatly increased response times to changes in oxygen concentration, while absolute sensitivity remained lower than those for **2**/PS blends. Having demon-

strated certain benefits of luminophore-attached sensors, we are currently investigating the generality of this effect by extending our study to more promising luminophores, including a number of iridium luminophores having both longer lifetimes and larger quantum yields than the complexes of the present study.

Acknowledgment. The authors thank Mr. Keith Bourque for his assistance in collecting the NMR spectra, Professor J. C. Scaiano of the University of Ottawa for his assistance in collecting lifetime and quantum yield data, and Dr. Youssef Mébarki for his assistance with the oxygen sensitivity experiments. M.C.D. and R.J.C. thank NSERC for a PGS B Scholarship and a Discovery Grant, respectively. P.J.M. thanks the Government of Ontario and Carleton University for an Ontario Graduate Scholarship. C.E.B.E. thanks the NRC for supporting this research through the Research Associate Program.

Supporting Information Available: Additional figures and crystallographic details. This material is available free of charge via the Internet at http://pubs.acs.org.

IC026230R